FLUIDIC CONTROL OF FLOW REGIME TRANSITION AND RETRANSITION IN A DUAL-BELL LAUNCHER NOZZLE

Brian Legros, Luc Léger, Azeddine Kourta, Abderrahmane Sefir, Mohamed Sellam, Amer Chpoun

FLUIDIC CONTROL OF FLOW REGIME TRANSITION AND RETRANSITION IN A DUAL-BELL LAUNCHER NOZZLE

ESTORIL, PORTUGAL | 09 – 13 MAY 2022

Brian Legros [1,2], Luc Léger [1], Azeddine Kourta [2], Abderrahmane Sefir [3], Mohamed Sellam [3], Amer Chpoun [3]

[1] National Centre for Scientific Research CNRS – Institute ICARE, Orléans, France, Email: brian.legros@cnrs-orleans.fr
[2] University of Orléans, INSA-CVL, PRISME, Orléans, France, Email: azeddine.kourta@univ-orleans.fr
[3] LMEE, Univ Evry, Université Paris-Saclay, Evry, France, Email: mohamed.sellam@univ-evry.fr

KEYWORDS: dual-bell nozzle, rocket nozzle, flow control

ABSTRACT:

Dual-bell nozzle (DBN) is a rocket nozzle concept that could provide substantial payload gain worth tens of millions of dollars. The control of transition, the reduction of side-loads, and the analysis of its stability have been the subject of numerous studies. The present paper focuses on the impact of radial secondary injection on DBN behaviour during its ascent and descent in the atmosphere. In the present study, the use of secondary injection allowed the transition nozzle pressure ratio to be increased by nearly 24% compared to a nozzle without any injection slot (smooth nozzle), and the lateral forces were reduced to less than 1% of the nozzle thrust. Finally, the jump in thrust during retransition was not found to be dependent on the secondary injection pressure, but was still reduced by over 61% compared to the smooth nozzle case.

1. INTRODUCTION

Nowadays, operating cost reduction and launchers efficiency enhancement have become crucial to reduce the cost of access to space for companies. The rising number of competitors in the astronautics industry have triggered well-off companies to decrease their service fee. Today's launchers such as Ariane 5 are using parallel staging which requires the first stage engine to be started before the lift off for security reasons [1]. As a consequence, the main stage engine faces off-design operating conditions during the rocket ascent, which induces high losses. As the nozzle geometry is fixed, the ambient pressure variation during the launcher's ascent imposes the flow inside the nozzle to be adapted for only one specific altitude. During the launcher's ascent, the nozzle experiences three distinct flow conditions: overexpansion, adapted flow, and underexpansion (see Figure 1). In order to prevent flow separation inside rocket nozzles which gives rise to flow instabilities and high side-loads at low altitude, the exit area has to be reduced, even if it implies lower performances at high altitude.

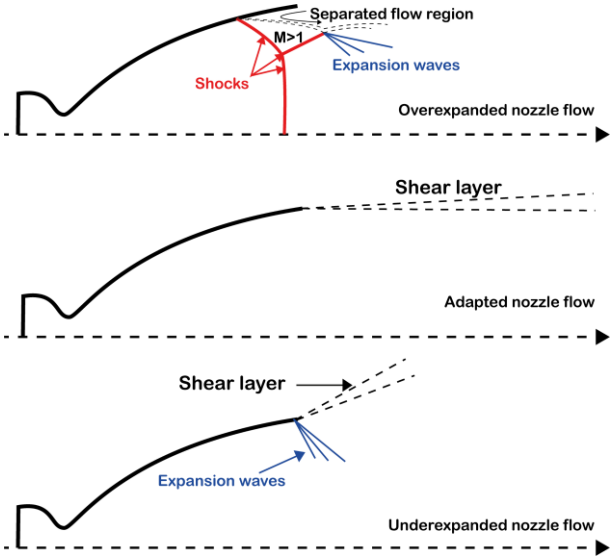

Figure 1: Conventional bell nozzle working modes.

The perfect nozzle would consist of a consistently increasing exit area to adapt to the varying pressure in the atmosphere during the ascent. However, this solution would considerably increase the complexity and reliability of the nozzle.

The dual-bell nozzle (DBN) was first mentioned by Swan [2] and later patented by Rocketdyne in 1968 [3]. The DBN concept consists of a converging/diverging nozzle, with a divergent section composed by two successive nozzle profiles of different expansion ratios: a small expansion ratio nozzle (base nozzle) to provide better performance at low altitude with little risks of side-loads, and a larger expansion ratio nozzle (extension nozzle) for better vacuum performance. The DBN geometry is illustrated in Figure 2. The two bell nozzles forming the divergent section are linked together through an inflection region. During sea-level mode, the flow separates from the nozzle wall

at the inflection point, providing a controlled, symmetric flow separation to limit the risks of lateral forces. As the launcher ascends into the atmosphere, the ambient pressure decreases and the flow will suddenly reattach in the extension nozzle, shifting the separation location at the nozzle exit, and providing better vacuum performance for high altitudes.
Figure 2 shows the two functioning modes of a DBN: low altitude mode, and high altitude mode.

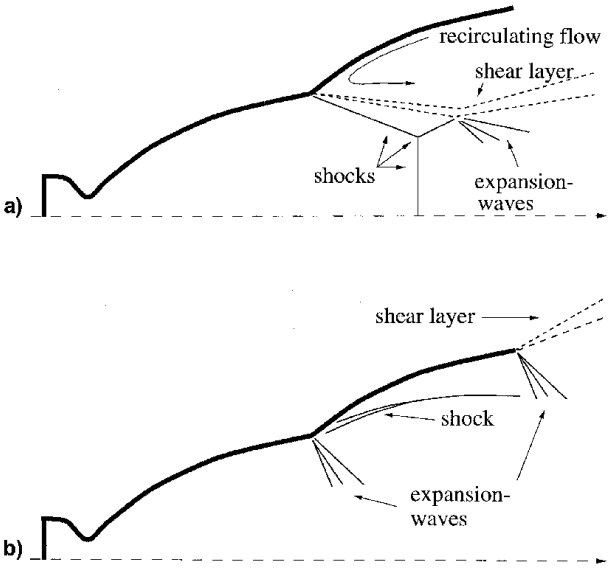

Figure 2: DBN low altitude mode and high altitude mode in a) and b) respectively [4].

Given the clear ability of dual-bell nozzles to reduce the cost of access to space, they became of more interest around the world, especially in Europe [5–9], Asia [10–12], and Russia [13,14].

Optimisation codes developed at the German Aerospace Center to quantify the financial gain on an Ariane-5-like launcher, with its Vulcain 2 engine mounted with a dual-bell nozzle, showed a payload mass gain into geostationary transfer orbit of 450kg [15]. A later study revealed a gain of 490kg [1], and more recently, an analysis performed by Ferrero [16] using similar conditions indicated a payload gain of 1.5 tons with the help of an optimised radial secondary injection to control the flow separation during the ascent.

Even though the DBN appears to be promising and easy to implement with no cooling issues, three main problems have to be carefully taken care of in order to make the DBN a viable concept: 1) Early transition and retransition Nozzle Pressure Ratio (NPR), 2) Lateral forces generation, 3) Stability.

As the presence of the extension corresponds to additional mass, the transition from low to high altitude mode (and vice versa) must take place as close to the optimum transition point (OTP) as possible to provide the best performances (see Figure 3). However, the natural transition and retransition in DBNs takes place earlier than the OTP (see Figure 3), hence, one should find a method to efficiently delay these critical phases. Moreover, the shift from one mode to the other produces undesirable side-loads caused by unsteady and asymmetrical flow separation that could be detrimental to the rocket integrity [17–19].

Transition in DBN depends on several parameters that are still the subject of numerous studies: Reynolds Number, testing environment, nozzle geometry, ambient pressure fluctuations, temperature etc. [19–24].

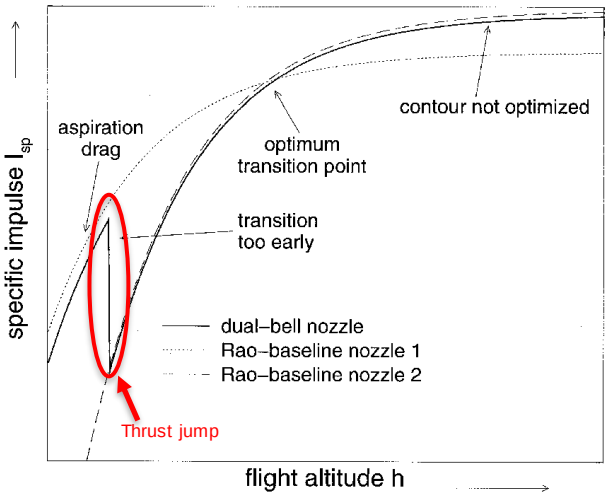

Figure 3: DBN efficiency compared to conventional nozzles inspired by [4].

The extension contour type is one of the key parameters to control the transition behaviour [25,26]. There are three different types of extension profiles: Negative wall Pressure gradient (NP), Positive wall Pressure gradient (PP), and Constant wall Pressure (CP).

In NP extension profiles, separation location was found to be dependent on the nozzle pressure ratio, and was well predicted by flow separation criterion such as the Schmucker's criterion [27–29]. No sudden transition is observed in NP extension profiles, and the slow movement of the separation front is the cause of important side-loads [9,27,30].

However, in the case of PP extension profiles and CP extension profiles, a sudden transition is observed experimentally [9], and numerically [31]. Thus, reducing the risks of side-loads generation [9,27,30].

The extension length also plays an important role on the performances of DBNs. Decreasing its length would decrease the lever arm, and consequently reduce the magnitude of the side-loads. However, decreasing the extension length also reduces the stability of the DBN with a smaller hysteresis [18], where the hysteresis is defined by the difference

between the transition NPR and the retransition NPR.

Extreme caution should be taken during DBN wind tunnel testing, as many studies demonstrated that DBNs behaved differently depending on whether the tests were performed in altitude chambers or at ambient conditions. Varying the feeding total pressure during experiments also greatly influences the behaviour of DBNs as it changes the Reynolds number and modifies the effective wall shape of the sensitive inflection region [22,25,32–34]. Though many of the previous studies provided significant information on DBN behaviour during the ascent and descent phases, only a few of them have focused on the control of transition and retransition, as well as side-loads generation in DBN.

Flow control in rocket nozzles has been the subject of numerous studies, whether to prevent flow separation in overexpanded nozzles at low altitude, to practise thrust vector control, or to decrease lateral forces amplitude on a launching pad [35–38]. In dual-bell nozzles, flow control has mainly been investigated by using film cooling and secondary injection in the perpendicular direction of the mainstream.
Film cooling in the vicinity of the inflection region showed a decrease in transition NPR in [39], but an increase for Proshchanka et al. in [40]. A reduction of thrust jump in the transition phases, and lower side-loads (an example of thrust jump is shown in Figure 3) were also reported. In [41], Martelli et al. indicated an effective capability of lowering the wall temperature at the cost of long-lasting lateral forces capable of exciting a nozzle structural mode.

In the second case, where radial fluidic injection is studied, significant gains could be found even for relatively small secondary mass flow rate. Indeed, a small percentage of the mainstream mass flow was sufficient for the secondary injection to increase the transition nozzle pressure ratio [42] when the injection was located downstream of the inflection point. As the ambient pressure starts to decrease and the transition from low-to-high altitude mode tends to happen, the radial injection of secondary fluid acts as an obstacle to the upstream flow, triggering a forced and symmetrical flow separation in the inflection region. The presence of the injection gives birth to a separation shock, in addition to the regular shock pattern visible in conventional dual-bell nozzle studies. Using the radial secondary injection, the flow will remain detached on a longer NPR range and bring one towards the optimum transition point [23,42,43]. Furthermore, radial secondary injection also has a positive impact side-loads reduction and stability as indicated in [44]. Indeed, a decrease in side-loads magnitude to the extent that the force balance could not capture the lateral forces anymore was observed in [44]. Secondary injection was also found to be useful to reduce the flip-flopping behaviour of the shock system during the retransition phases, where the flip-flopping phenomenon corresponds to a high amplitude and unsteady displacement of the separation point. In this paper, the authors study the influence of the secondary injection cavity volume (see Figure 6), and the impact of the secondary pressure ratio (SPR) on dual-bell nozzle behaviour during the ascent and descent phases of a rocket in the atmosphere.

2. EXPERIMENTAL SETUP

The experiments were performed in the EDITH wind tunnel (WT) (see Figure 4), at the institute ICARE, of the National Centre for Scientific Research. The test facility was the same as described in [52]**.** Dry air from 320 litre tanks and pressurised at 300 bar is adjusted to 3.5 bar to serve as the nozzle feeding total pressure. Then, the air travels through the dual-bell nozzle and exits in the depressurised WT test section. The pressure inside the test section is controlled by a 345 kW pumping group and by a valve located in the WT diffuser. The opening, and closing of this valve allows one to decrease, and increase the pressure inside the WT test section. During the experiments, the dual-bell nozzle is mounted on a force balance designed by the authors and which moves freely along the orthogonal axis (x,y,z). The thrust and lateral forces are measured by the force balance using four HBM S2M S-shaped strain-gauge force transducers, whose signals are amplified to a 0-10 V range before its acquisition from the SCXI-1140 card, at 1 kHz. Two transducers of 200 N located on both sides of the force balance were used to measure the vertical force component; one 200 N transducer measured the nozzle thrust; and a 20 N transducer measured the lateral forces.

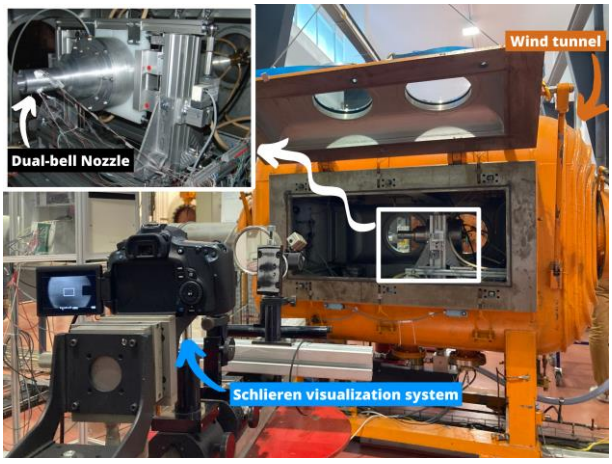

Figure 4: EDITH wind tunnel testing facility.

The base nozzle was designed as a truncated ideal contour (TIC) for an exit Mach number of 3.2, and the extension nozzle was built as a constant pressure (CP) extension profile. To actively control the flow transition and retransition behaviour, a

secondary fluid was radially injected in the extension part of the DBN. The 2 mm width injection slot was made possible by manufacturing the DBN in two parts, and the slot was placed 8 mm downstream of the inflection point. This technique also allowed the creation of a settling chamber for the secondary injection (called cavity, visible in Figure 5), to provide an axisymmetric, homogeneous secondary injection.

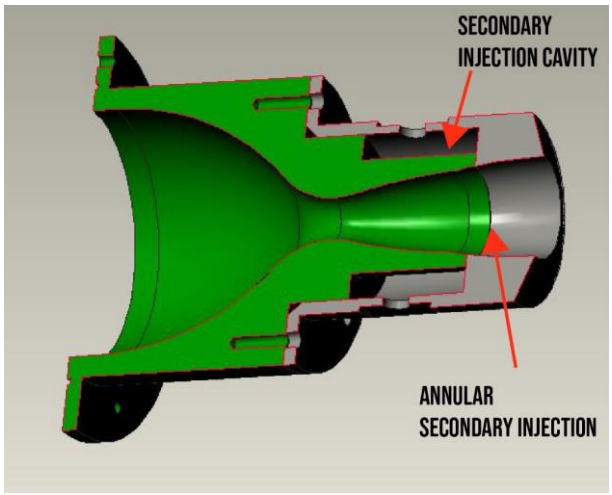

Figure 5: DBN geometry with secondary injection cavity.

In this study, two test campaigns have been carried out. The first one was performed without injecting a secondary fluid as it allowed the authors to investigate the influence of the cavity volume on DBN transition behaviour. In this campaign, a cylinder was manufactured to be inserted into the cavity in order to provide a smaller secondary chamber volume compared to the original cavity. The second test campaign explored the impact of the secondary pressure ratio (SPR) on DBN transition behaviour. In this case, multiple secondary injection pressures were used: 0.3, 0.5, 0.7, and 0.9 bar, corresponding to a SPR of 8.6%, 14.3%, 20.0%, and 25.7%, and equivalent to a theoretical mass flow rate of 1.61 g/s, 2.68 g/s, 3.75 g/s, and 4.82 g/s. The ratio between the secondary injection mass flow and the mainstream mass flow for the different secondary pressures were respectively 0.9%, 1.4%, 2.0%, 2.6%.

For all experiments, the DBN main settling pressure was kept constant at 3.5 bar and the ambient pressure was varied using the pumping group to trigger transition and retransition in the DBN. When secondary injection was used, the injection pressure was kept constant throughout the experiment. The ambient pressure and the secondary feeding total pressure inside the cavity were measured using Kulite® XCQ-062 pressure transducers of 0-100kPa range. Geometrical details of the DBN profile obtained by an in-house code based on the method of characteristics are presented in Figure 6, and the reader can find further details in [52].

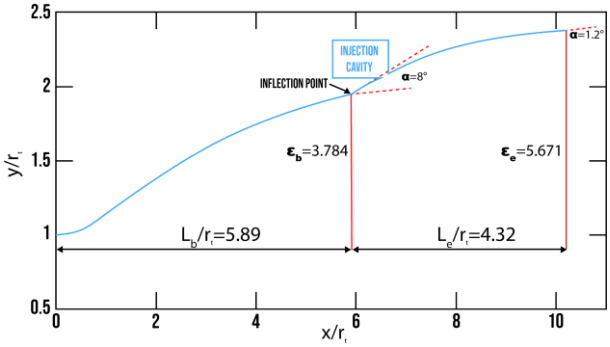

Figure 6: Geometrical parameters of the DBN profile used during the test campaign.

3. RESULTS AND DISCUSSIONS

3.1. Cavity effects on dual-bell nozzle behaviour

The secondary injection inside the divergent section of a dual-bell nozzle requires an external cavity to set the stagnation conditions for the secondary jet (see Figure 5). However, the effect of the cavity has not been the subject of study. This section aims to provide an insight of the injection cavity volume effect on transition and retransition behaviour in DBNs. To do so, 4 different experiments were performed in the EDITH depressurized WT using: 1) a DBN with no injection slot called smooth nozzle; 2) a DBN with an injection slot and an empty cavity; 3) a DBN with an injection slot and a cavity inside which a cylinder had been inserted to decrease its volume; 4) a DBN with an injection slot and an empty cavity connected to the secondary injection pipes, but without any secondary injection. The empty cavity, the filled cavity, and the empty cavity connected to the injection pipes have respectively an internal volume of 89.8 cm^3, 30.1 cm^3, and 558.8 cm^3.

For each configuration, the experiments were performed so as to provide an average of fourteen transitions and retransitions phases per test, and to allow the calculation of the standard deviation. Figure 7 shows the evolution of the thrust, NPR, and side-loads during a classic run of the wind tunnel for the empty cavity connected to the injection pipes but without any secondary injection configuration.

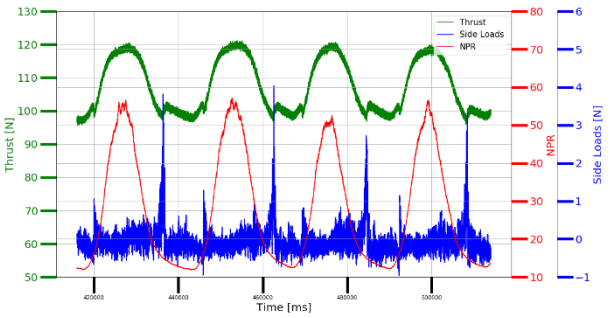

Figure 7: Evolution of the thrust, NPR, and side-loads as a function of time during an experiment of DBN with cavity connected to the injection pipes,

but without any secondary injection.

The EDITH WT happened to be a true asset when it comes to repeatability and reliability of the measurements. Before NPR=15, the dual-bell nozzle functions in the low altitude, overexpanded mode, where separation is located in the vicinity of the inflection point, ahead of an oblique separation shock. As the NPR is increased, the thrust generated by the nozzle also increases until a sudden drop in thrust occurs at NPR=15.14 (see Figure 7). At this specific NPR, the transition takes place and the separation front moves from the inflection to the nozzle exit, switching the DBN mode from low, to high altitude. During the transition, the separation front movement, along with its uneven wall pressure distribution for a given streamwise location produces lateral forces, as seen in Figure 7. Starting from the high-altitude mode, as the NPR is reduced, the thrust also decreases until NPR=14.3. If the NPR keeps decreasing, a sudden jump in thrust is achieved at NPR=14.4, arising from the retransition from high to low altitude mode. In this case, the separation front moves back, from the nozzle exit, to the inflection point. Similarly, the separation front movement generates lateral forces, which are higher during retransition than during transition.

Once the experiments were carried out for the four cases (smooth, empty cavity, empty cavity with injection pipes, and filled cavity nozzles), the following parameters were used to study the effects of the presence of the cavity in the DBN during transitions and retransitions: a) transition NPR; b) maximum side-loads magnitude peak; c) thrust jump (see thrust jump example in Figure 3). Figure 8 shows the transition and retransition NPR for the smooth DBN and the three DBN cavity configurations. It shows that the cavity volume does not significantly impact the retransition NPR compared to the smooth nozzle. Nevertheless, the presence of the cavity generates a slightly greater transition NPR, though the difference between the filled cavity, and the empty cavity, is not clearly noticeable. The very small air pocket volume in the filled cavity case also implies that the simple presence of the injection slot is sufficient to delay transition. Indeed, the injection slot seems to act as an obstacle which maintains the separation location fixed during a short time, inducing a slightly greater transition NPR. However, in the case where the injection pipes were mounted on the cavity, a larger increase in transition NPR becomes visible compared to all the other cases and the transition NPR increases by 7.3% with respect to the smooth nozzle configuration. This result suggests that the air pocket volume inside the cavity plays a role in DBNs transition behaviour, as the emptying of this bigger volume during the ascent could interfere with the flow at the separation location and delay transition. While the retransition NPR remains fairly unchanged between the smooth nozzle, and the two smallest cavity volume configurations, the increase in transition NPR brings the hysteresis from 2.1% for the smooth nozzle, to 4.6% and 4.9% for the filled, and empty cavity, respectively. In the last case, the retransition NPR is slightly increased, but in less proportion than the transition NPR, bringing the hysteresis to 7%. Therefore, the existence of an injection slot, and the volume of air inside the cavity volume not only grants a delay in transition NPR, but also increases the stability of the DBN.

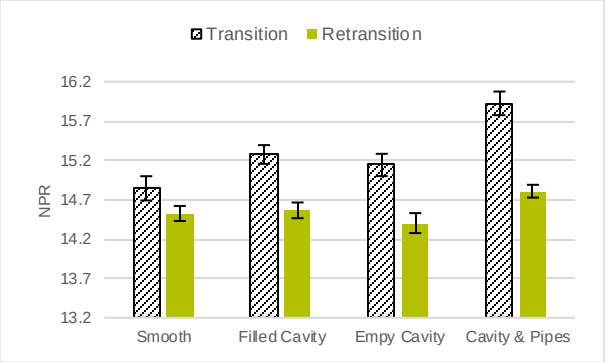

Figure 8: Transition and retransition NPR for the smooth nozzle and the different cavity configurations. Error bars show the standard deviation calculated for each configuration.

Similar to the previous analysis on retransition NPR, the influence of the cavity volume on side-loads generation during retransition could not clearly be identified in Figure 9, where the maximum lateral forces during transition and retransition for every configuration is displayed. For the smooth, empty cavity, and cavity with pipes DBN configurations, Figure 9 shows similar side-loads magnitudes during retransition. The larger peak (4.4 N) during retransition phases for the filled cavity configuration compared to the other cases is mainly attributed to harsher manual corrections to maintain the feeding total pressure of 3.5 bars.

However, the presence of a cavity induced a decrease exceeding 50% in lateral forces generation during transition for the two biggest cavity volume configurations, with a maximum decrease of 55.6% in the empty cavity case. The lateral forces reductions might emanate from the more symmetrical flow separation created by the presence of the injection slot located downstream of the inflection region. Even though the decrease in side-loads with the help of the injection slot and the cavity is clear during the transition process, the impact of the volume of air inside the cavity remains uncertain, especially between the empty cavity and the cavity with pipes.

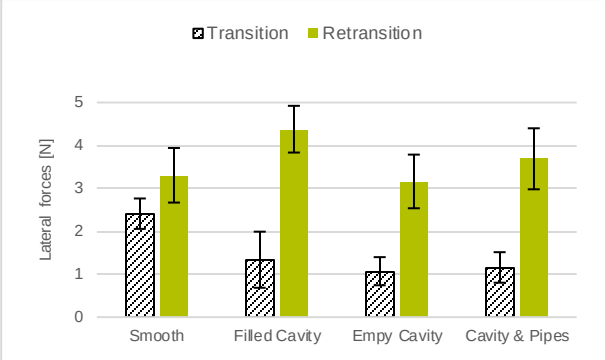

Figure 9: Maximum lateral forces generated during transition and retransition for the smooth nozzle and the different cavity cases. Error bars show the standard deviation calculated for each configuration.

During the transition and retransition phases, the movement of the separation front from the inflection region to the extension exit (and vice versa) induces a thrust jump (see Figure 3). The jumps are caused by the sudden change in nozzle area ratio and can be dangerous for the rocket, especially for single-stage-to-orbit (SSTO) vehicles. Figure 10 shows the absolute values of thrust jump during transition and retransition. The experiments revealed a decrease in both parameters with an increase in cavity volume. During the ascent phase, the thrust jump was reduced by over 45.5% in the cavity with pipes case compared to the smooth nozzle. The thrust jump during the descent was decreased in less proportion than during the ascent, as it dropped at best by 19.1%. The corresponding findings are in accordance with the theory as the presence of the cavity delays the transition NPR, the sudden jump in performances is reduced during the ascent.

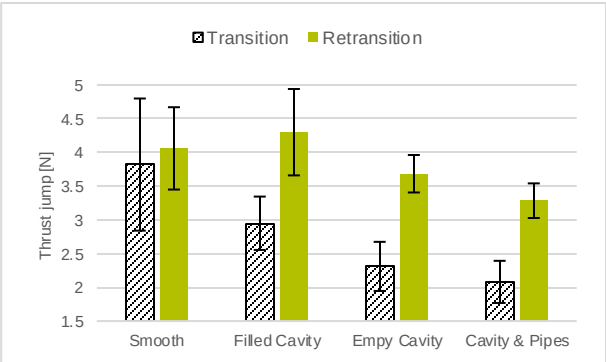

Figure 10: Thrust jump during transition and retransition for the smooth nozzle and the different cavity cases. Error bars show the standard deviation calculated for each configuration.

3.2. Secondary injection effects on dual-bell nozzle behaviour

This section consists in analysing the influence of the secondary injection pressure on the DBN transition, and retransition behaviour. During this test campaign, the total feeding pressure and the injection pressure were kept constant, while the ambient pressure in the wind tunnel was repetitively increased and decreased to trigger the transitions and retransitions inside the DBN. Figure 11 shows the evolution of the measured parameters during a typical experiment using a secondary injection pressure of 0.7 bar. The processes of transition and retransition are similar to the ones observed in the cavity influence study, and have already been described in Sec. 3.1. Four different secondary injection pressures were used for this study: 0.3, 0.5, 0.7, and 0.9 bar, which correspond to a secondary pressure ratio (SPR) of 8.6%, 14.3%, 20%, and 25.7% respectively. Figure 12 shows the evolution of the transition and retransition NPR as a function of secondary injection pressure. The 5th injection case, associated with a pressure of 0 bar on Figure 12, Figure 13, and Figure 14, corresponds to the case with the empty cavity connected with the injection pipes, but without any injection.

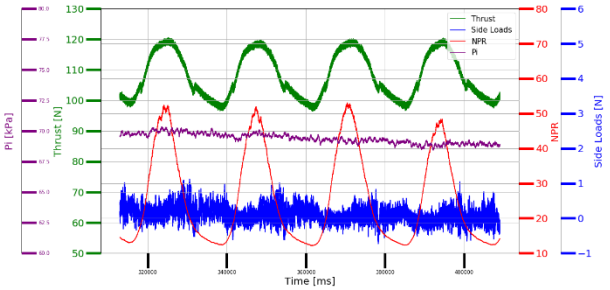

Figure 11: Evolution of the thrust, NPR, side-loads, and secondary injection pressure as a function of time during an experiment of DBN with a secondary injection pressure of 0.7 bar.

The experiment confirms that the SPR greatly increases the transition, and retransition NPR (see Figure 12). As the SPR is increased, the transition and retransition NPR are respectively increased between 8.2% to 15.5% and between 13.3% to 17.3% compared to the configuration with the cavity connected with the injection pipes (but without any injection). The increase in transition and retransition NPR was even more evident when compared to the smooth nozzle case: 23.9% and 19.6% at best respectively. The hysteresis was the highest for the cavity with no injection (reaching 7%), then decreased to 2.7% for Pi=0.3 bar, and progressively increased along with the secondary injection pressure to hit a maximum of 5.7% for Pi=0.7 bar. It is worth mentioning that the secondary flow was not injected at a sonic speed in the case of Pi=0.3 bar. Therefore, the influence of the subsonic jet may have played a role in the early retransition in this specific case, as the cavity is free to suck or blow air freely in the vicinity of the injection slot region.

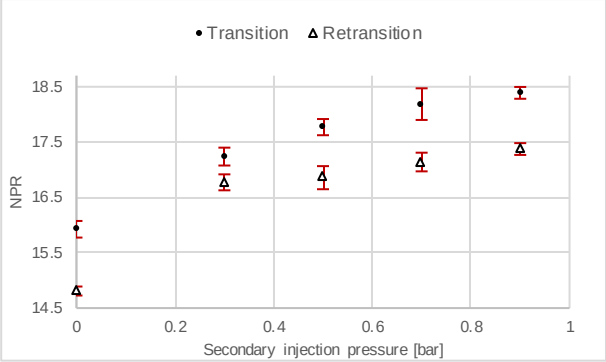

Figure 12: Transition and retransition NPR as a function of secondary injection pressure. Error bars show the standard deviation calculated for each configuration.

The lateral forces (in Figure 13) are dramatically decreased in the presence of secondary injection. From SPR=14.3% and above, the decrease in side-loads magnitude is such that the force balance is not capable of capturing the different peaks, as they fall into the measurement noise, ± 0.5 N caused by the pumping group (see Figure 11). Let us define the ratio between the maximum side-loads magnitude and the thrust just before the transition takes place as: SLR_{trans}. The same ratio can be defined for retransition phases: $SLR_{retrans}$. In the smooth nozzle configuration, the SLR_{trans} reaches 2.4%, while the simple presence of the cavity connected to the injection pipes without any injection allows a decrease in SLR_{trans} so as to reach 1.1%. Eventually, once secondary injection is used for SPRs of 8.6% and above, the SLR_{trans} drops below 1%.

During retransition, lateral forces have always been more important than during transition. Indeed, the $SLR_{retrans}$ hits 3.4% in the smooth nozzle configuration, but secondary injection usage reduces the $SLR_{retrans}$ below 1% for SPRs of 14.3% and above, providing over three times lower lateral forces compared to the smooth nozzle configuration.

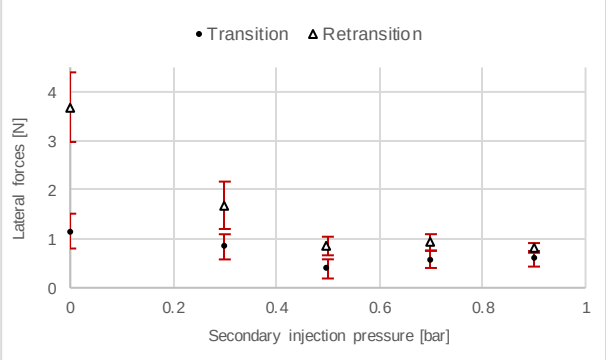

Figure 13: Maximum lateral forces generated during transition and retransition as a function of secondary injection pressure. Error bars show the standard deviation calculated for each configuration.

The influence of secondary injection on thrust jump during transition and retransition are showed in Figure 14. The test series revealed that the secondary injection pressure did not present any significant impact on the thrust jump magnitude during transition and retransition as it becomes fairly constant from Pi=0.5 bar. For Pi=0.3 bar, the jump magnitudes during both, the ascent and the descent, are slightly higher than for the other injection pressures. The latter observation might be influenced by the non-sonic secondary injection and a more thorough investigation is necessary to validate this hypothesis.

However, on comparing the smooth nozzle case to the injection cases, the presence of the injection jet induced a decrease in thrust jump during transition by a factor of 2. Figure 14 also reveals that no significant differences were measured between the cavity connected to the injection pipes configuration and the different injection cases during transition.

Nonetheless, the presence of secondary injection reduces the thrust jump during retransition up to 51.9% compared to the cavity with pipes case, and 61.1% compared to the smooth nozzle. The previous results would be extremely suitable, should dual-bell nozzles with secondary injection be used in reusable launcher vehicles. Indeed, the descent of the different stages of the rocket would have to go from high altitude mode, to low altitude mode. The secondary injection, with its capabilities for decreasing lateral forces and sudden change in nozzle thrust while improving nozzle efficiency, could therefore be seen as a genuine asset for the next generation of reusable launchers.

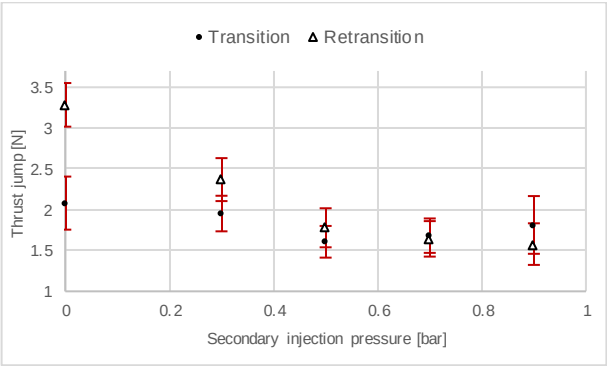

Figure 14: Thrust jump during transition and retransition as a function of secondary injection pressure. Error bars show the standard deviation calculated for each configuration.

Secondary injection is therefore beneficial in dual-bell nozzles as, not only does it delay the transition NPR and considerably reduce side-loads during both, transition and retransition, but it also decreases the sudden thrust jumps during the ascent and the descent of a launcher. The previous findings are particularly interesting for SSTO launchers, and reusable launching vehicles.

4. CONCLUSION

This paper focused on two subjects: the influence of the injection cavity volume and the impact of radial secondary injection on DBN transition behaviour. The first test campaign revealed that the cavity volume did not have a significant impact on DBN retransition NPR or side-loads generation during the descent phases. However, the presence of the cavity clearly influences side-loads generation during transition as the lateral forces were reduced by over 50% in the two biggest cavity volume configurations. The latter observation is attributed to the controlled and symmetric flow separation made possible by the presence of the injection slot and cavity located downstream of the inflection region. The same behaviour was observed for the thrust jump during transition, where the magnitudes of the jumps were reduced by 45% for the biggest cavity volume configuration.

When secondary injection was tested, four different pressure values ranging from 0.3 bar to 0.9 bar were used. The maximum secondary injection pressure used generated an increase in transition nozzle pressure ratio of nearly 24% compared to a nozzle not mounted with a secondary injection slot (smooth nozzle). The lateral forces were also decreased below 1% of the nozzle thrust during both: transition, and retransition phases using a secondary mass flow of only 1.4% of the mainstream mass flow. Moreover, secondary injection reduced the thrust jump during retransition by over 61% for a secondary pressure of 0.9 bar compared to the smooth nozzle case.

The impact of higher secondary injection pressures will be investigated in future work to optimise the performances of the dual-bell nozzle. A numerical work is also underway to sustain experimental findings.

5. Acknowledgments

We would like to gratefully acknowledge the laboratory of Excellence CAPRYSSES framework and the financial support of this study from Grant No. ANR-11-LABX-0006-01 of the Investissements d'Avenir LabEx CAPRYSSES. We would also like to thank Nicolas Gouillon for his technical assistance and Matthieu Sammut for his assistance during patent filing.

6. REFERENCES

1. Stark, R.; Génin, C.; Schneider, D.; Fromm, C. Ariane 5 Performance Optimization Using Dual-Bell Nozzle Extension. *Journal of Spacecraft and Rockets* **2016**, *53*, 743–750, doi:10.2514/1.A33363.
2. Walter .C, S. The Influence of Nozzle Design on the Flight Performance of Rocket Vehicles, with an Analysis of the Results of Jet Separation, 1948.
3. Sutor, A.T. 1968_Sutor-PATENT_READ 1968.
4. Hagemann, G.; Immich, H.; Nguyen, T. van; Dumnov, G.E. Advanced Rocket Nozzles. *JOURNAL OF PROPULSION AND POWER* **1998**, *14*, 620–634.
5. Immich, H.; Caporicci, M. Festip Technology Developments in Liquid Rocket Propulsion for Reusable Launch Vehicles. In Proceedings of the 32nd Joint Propulsion Conference and Exhibit; American Institute of Aeronautics and Astronautics Inc, AIAA, 1996; pp. 1–14.
6. Hagemann, G.; Frey, M.; Manski, D. A Critical Assessment of Dual-Bell Nozzles. In Proceedings of the 33rd Joint Propulsion Conference and Exhibit; American Institute of Aeronautics and Astronautics Inc, AIAA, 1997.
7. Haidinger, F.A.; Gorgen', J.; Haeseler, D. Numerical Prediction of Flow Separation for Advanced Nozzle Concepts. In Proceedings of the 34th AIAA/ASME/SAE/ASEE; 1998.
8. Frey, M.; Hagemann, G. Critical Assessment of Dual-Bell Nozzles. *Journal of Propulsion and Power* **1999**, *15*, 137–143, doi:10.2514/2.5402.
9. Hagemann, G.; Terhardt, M.; Haeseler, D.; Frey, M. Experimental and Analytical Design Verification of the Dual-Bell Concept. *Journal of Propulsion and Power* **2002**, *18*, 116–122, doi:10.2514/2.5905.
10. Kumakawa, A.; Tamura, H.; Niino, M.; Nosaka, M.; Yamada, H.; Kanmuri, A.; Konno, A.; Atsumi, M. Propulsion Research for Rocket SSTOs at NAL/KRC. In Proceedings of the 35th AIAA/ASME/SAE/ASEE Joint Propulsion Conference and Exhibit; 1999.
11. Kusaka, K.; Kumakawa, A.; Niino, M.; Konno, A.; Atsumi, M. Experimental Study on Extendible and Dual-Bell Nozzles under High Altitude Conditions. In Proceedings of the 36th AIAA/ASME/SAE/ASEE Joint Propulsion Conference and Exhibit; 2000.
12. Miyazawa, M.; Takeuchi, S.; Takahashi, M. Flight Performance of Dual-Bell Nozzles. In Proceedings of the 40th AIAA Aerospace Sciences Meeting and Exhibit; 2002.
13. Goncharov, N.S.; Orlov, V.A.; Rachuk, V.S.; Shostak, A. v; Starke, R. Reusable Launch Vehicle Propulsion Based on the RD-0120 Engine. In Proceedings of the 31st AIAA/ASME/SAE/ASEE Joint Propulsion Conference and Exhibit; 1995.
14. Dumnov, G.E.; Ponomaryov, N.B.; Voinov, A.L. Dual Bell Nozzles for Rocket Engines of Launch Vehicle Upper Stages and Orbital Transfer Vehicles. In Proceedings of the 33rd Joint Propulsion Conference and Exhibit; American Institute of Aeronautics and Astronautics Inc, AIAA, 1997.

15. Schneider, D.; Génin, C.; Stark, R.; Fromm, C.M. Ariane 5 Performance Optimization Using Dual Bell Nozzle Extension. In Proceedings of the 4th Space Propulsion Conference; 2014.
16. Ferrero, A.; Conte, A.; Martelli, E.; Nasuti, F.; Pastrone, D. Dual-Bell Nozzle with Fluidic Control of Transition for Space Launchers. *Acta Astronautica* **2022**, *193*, 130–137, doi:10.1016/j.actaastro.2021.12.048.
17. Nürnberger-Genin, C.; Stark, R. Flow Transition in Dual Bell Nozzles. *Shock Waves* **2009**, *19*, 265–270, doi:10.1007/s00193-008-0176-4.
18. Génin, C.; Stark, R.H. Side Loads in Subscale Dual Bell Nozzles. *Journal of Propulsion and Power* **2011**, *27*, 828–837, doi:10.2514/1.B34170.
19. Stark, R.; Génin, C. Scaling Effects on Side Load Generation in Subscale Rocket Nozzles. In Proceedings of the 52nd AIAA/SAE/ASEE Joint Propulsion Conference, 2016; American Institute of Aeronautics and Astronautics Inc, AIAA, 2016.
20. Génin, C.; Stark, R.; Haidn, O.; Quering, K.; Frey, M. Experimental and Numerical Study of Dual Bell Nozzle Flow. In Proceedings of the 4thEuropean conference for aerospace sciences; EDP Sciences, June 2013; pp. 363–376.
21. Génin, C.; Gernoth, A.; Stark, R. Experimental and Numerical Study of Heat Flux in Dual Bell Nozzles. In Proceedings of the American Institute of Aeronautics and Astronautics; 2013.
22. Verma, S.B.; Stark, R.; Haidn, O. Gas Density Effects on Dual-Bell Transition Behavior. *Journal of Propulsion and Power* **2012**, *28*, 1315–1323, doi:10.2514/1.B34451.
23. Zmijanovic, V.; Leger, L.; Sellam, M.; Chpoun, A. Assessment of Transition Regimes in a Dual-Bell Nozzle and Possibility of Active Fluidic Control. *Aerospace Science and Technology* **2018**, *82–83*, 1–8, doi:10.1016/j.ast.2018.02.003.
24. Génin, C.; Stark, R. Experimental Investigation of the Inflection Geometry on Dual Bell Nozzle Flow Behavior. In Proceedings of the 47th AIAA/ASME/SAE/ASEE Joint Propulsion Conference & Exhibit; 2011.
25. Nasuti, F.; Onofri, M.; Martelli, E. Role of Wall Shape on the Transition in Axisymmetric Dual-Bell Nozzles. *Journal of Propulsion and Power* **2005**, *21*, 243–250, doi:10.2514/1.6524.
26. Kimura, T.; Niu, K.; Yonezawa, K.; Tsujimoto, Y. Experimental and Analytical Study for Design of Dual-Bell Nozzles. In Proceedings of the 45th AIAA/ASME/SAE/ASEE Joint Propulsion Conference & Exhibit; 2009.
27. Tomita, T.; Takahashi, M.; Sasaki, M.; Tamura, H. Investigation on Characteristics of Conventional-Nozzle-Based Altitude Compensating Nozzles by Cold-Flow Tests. In Proceedings of the 42nd AIAA/ASME/SAE/ASEE Joint Propulsion Conference & Exhibit; 2006.
28. Schmucker, R.H. *Flow Processes in Overexpanded Chemical Rocket Nozzles. Part 1: Flow Separation*; 1984;
29. Stark, R. Flow Separation in Rocket Nozzles – an Overview. In Proceedings of the 49th AIAA/ASME/SAE/ASEE Joint Propulsion Conference; American Institute of Aeronautics and Astronautics Inc., 2013; Vol. 1 PartF, pp. 1–10.
30. Horn, M.; Fisher, S. *Dual-Bell Altitude Compensating Nozzles*; 1993;
31. Nasuti, F.; Onofri, M.; Martelli, E. Numerical Study of Transition between the Two Operating Modes of Dual-Bell Nozzles. In Proceedings of the 38th AIAA/ASME/SAE/ASEE; 2002.
32. Verma, S.B.; Stark, R.; Haidn, O. Reynolds Number Influence on Dual-Bell Transition Phenomena. *Journal of Propulsion and Power* **2013**, *29*, 602–609, doi:10.2514/1.B34734.
33. Martelli, E.; Nasuti, F.; Onofri, M. Numerical Parametric Analysis of Dual-Bell Nozzle Flows. *AIAA Journal* **2007**, *45*, 640–650, doi:10.2514/1.26690.
34. Stark, R.; Génin, C. Flow Separation in Rocket Nozzles under High Altitude Condition. *Shock Waves* **2016**, *27*, 63–68, doi:10.1007/s00193-016-0631-6.
35. Mockenhaupt, J.D. Cold Flow Tests with Chamber-Bleed Gas Injection Thrust Vector Control. *Aerojet technology* **1988**, *4*, 14–23, doi:10.2514/6.1988-3334.
36. Zmijanovic, V. Secondary Injection Fluidic Thrust Vectoring of an Axisymmetric Supersonic Nozzle, 2013.
37. Zmijanovic, V.; Leger, L.; Depussay, E.; Sellam, M.; Chpoun, A. Experimental-Numerical Parametric Investigation of a Rocket Nozzle Secondary Injection Thrust Vectoring. *Journal of Propulsion and Power* **2016**, *32*, 196–213, doi:10.2514/1.B35721.
38. Stark, R.H.; Génin, C. Experimental Study on Rocket Nozzle Side Load Reduction. *Journal of Propulsion and Power* **2012**, *28*, 307–311, doi:10.2514/1.B34253.
39. Schneider, D.; Stark, R.; Génin, C.; Oschwald, M.; Kostyrkin, K. Active Control of Dual-Bell Nozzle Operation Mode Transition by Film Cooling and Mixture Ratio Variation. In Proceedings of the Journal of Propulsion and Power; American Institute of Aeronautics and Astronautics Inc., 2019;

Vol. 36, pp. 47–58.
40. Proshchanka, D.; Yonezawa, K.; Koga, H.; Tsujimoto, Y.; Kimura, T.; Yokota, K. Control of Operation Mode Transition in Dual-Bell Nozzles with Film Cooling. *Journal of Propulsion and Power* **2012**, *28*, 517–529, doi:10.2514/1.B34202.
41. Martelli, E.; Nasuti, F.; Onofri, M. Numerical Analysis of Film Cooling in Advanced Rocket Nozzles. *AIAA Journal* **2009**, *47*, 2558–2566, doi:10.2514/1.39217.
42. Léger, L.; Zmijanovic, V.; Sellam, M.; Chpoun, A. Controlled Flow Regime Transition in a Dual Bell Nozzle by Secondary Radial Injection. *Experiments in Fluids* **2020**, *61*, doi:10.1007/s00348-020-03086-3.
43. Ferrero, A.; Martelli, E.; Nasuti, F.; Pastrone, D. Fluidic Control of Transition in a Dual-Bell Nozzle. In Proceedings of the AIAA Propulsion and Energy 2020 Forum; American Institute of Aeronautics and Astronautics Inc, AIAA, 2020; pp. 1–11.
44. Léger, L.; Zmijanovic, V.; Sellam, M.; Chpoun, A. Experimental Investigation of Forced Flow Regime Transition in a Dual Bell Nozzle by Secondary Fluidic Injection. *International Journal of Heat and Fluid Flow* **2021**, *89*, doi:10.1016/j.ijheatfluidflow.2021.108818.